JOURNAL OF OCULAR PHARMACOLOGY AND THERAPEUTICS
Volume 32, Number 5, 2016

DOI: 10.1089/jop.2015.0134

Immunosuppressive Treatment Can Alter Visual Performance in the Royal College of Surgeons Rat

Ann E. Cooper,[1] Jang-Hyeon Cho,[2] Steven Menges,[2] Sahar Masood,[2] Jun Xie,[2] Jing Yang,[2] and Henry Klassen[2]

Abstract

Purpose: Immunosuppression is frequently employed to enhance survival of xenografted human cells as part of translational proof-of-concept studies. However, the potential effects of this treatment are easily overlooked.
Methods: As part of baseline testing in the dark-eyed variant of the dystrophic Royal College of Surgeons (RCS) rat, we documented the time course of retinal degenerative changes versus Long Evans controls using bright field retinal imaging, fluorescein angiography, and histology and examined the impact of immunosuppression on visual function. Rats received either no treatment or systemic immunosuppression with oral cyclosporine A and injectable dexamethasone and subsequently underwent functional evaluation by optomotor response testing and electroretinography (ERG) at multiple intervals from P45 to P180.
Results: Immunosuppressed RCS animals demonstrated poorer performance on functional tests than age-matched untreated rats during the earlier stages of degeneration, including significantly lower spatial acuities on optomotor threshold testing and significantly lower b-wave amplitudes on scotopic and photopic ERGs. Retinal imaging documented the progression of degenerative changes in the RCS fundus and histologic evaluation of the RCS retina confirmed progressive thinning of the outer nuclear layer.
Conclusions: A standard regimen of cyclosporine A plus dexamethasone, administered to RCS rats, results in demonstrable systemic side effects and depressed scores on behavioral and electrophysiological testing at time points before P90. The source of the functional impairment was not identified. This finding has implications for the interpretation of data generated using this commonly used translational model.

Introduction

Animal models of human disease play a critical role in both discovery research and subsequent translational development of cell-based therapeutics, including those intended for treatment of blinding retinal diseases such as retinitis pigmentosa (RP) and age-related macular degeneration. Rodent models of retinal degeneration are commonly used to evaluate the potential of stem cell-based therapeutics and establish proof-of-concept as part of investigational new drug (IND)-enabling studies,[1] or the equivalent outside of the United States.[2]

Multiple cell-based projects for the retina have now successfully transitioned from preclinical stages into clinical trials based in part on such studies[3] and in many cases the Royal College of Surgeons (RCS) rat was selected as the model of choice for functional testing. The RCS rat is a popular and relatively well-characterized model of retinal dystrophy. The underlying mutation is in the *MERTK* gene, resulting in defective phagocytotic activity by the retinal pigment epithelium and accumulation of shed photoreceptor outer segments. The accumulated debris leads to eventual photoreceptor cell death and loss of visual function. By way of example, this rodent model was used in the recent xenotransplantation studies[4] used to support a clinical stem cell-based approach for macular degenerative diseases.[5,6]

A major challenge confronting translational stem cell projects for retinal degeneration is that using the RCS rat to validate the efficacy of human cell products represents xenotransplantation. Even in a so-called ''immune-privileged site'' such as the eye, systemic immunosuppression is required for long-term survival of human grafts. While this might reflect in part readily identifiable triggers such as a breakdown of intraocular barriers during cell delivery,[7] based on our experience the specific mechanisms underlying xenograft tolerance[8] or rejection[9] in the posterior segment of the

[1]William R. Pritchard Veterinary Medical Teaching Hospital, School of Veterinary Medicine, University of California-Davis, Davis, California.
[2]Gavin Herbert Eye Institute, Stem Cell Research Center, University of California, Irvine, California.

eye are likely complex, atypical, and not easily delineated.[10] Until such mechanisms are adequately understood and addressed, or immunocompromised versions of disease models are developed, systemic immunosuppression will remain an important adjunct to the development of cell therapies.

An established method for immunosuppression in the RCS rat involves the sustained use of cyclosporine A, a nonsteroidal inhibitor of T-lymphocyte function, in combination with shorter term use of dexamethasone, a synthetic glucocorticoid and ACTH inhibitor.[11] This protocol has shown success for a range of human cell types in the eye, specifically for preventing rejection in xenograft recipients over the long term time courses needed for *in vivo* validation of therapeutics aimed at retinal degenerations. Although cyclosporine A is more traditionally administered as a sole agent, studies have supported the synergistic effects of glucocorticoids and cyclosporine A on tumor necrosis factor-alpha-induced endothelial cell activation when administered in combination to xenograft recipients.[12]

Our laboratory's primary focus has involved the development and evaluation of retinal progenitor cell therapy in RCS rats as a model for therapeutic intervention in humans with RP. Over the course of this work we have generated a normative database of RCS and Long Evans rat anatomical and functional data. Evaluation of this data revealed an impact of systemic immunosuppressive treatment on functional visual performance in the RCS rat at specific time points. The observations described here may be of interest to other investigators in the field because of the potential implications for interpretation of *in vivo* product potency data during preclinical testing.

Methods

Animals

A total of 116 dystrophic RCS rats (rdy+ p+) and 42 Long Evans wild-type control rats were used for this study. All animals were pigmented with the brown-eyed, dark-hooded RCS phenotype. The rats were bred in a colony at the University of California, Irvine, and maintained under a 12-h light/dark cycle (maximum 7.7 lux at cage level). Animals were housed and handled in adherence with guidelines set forth by the Institutional Care and Use Committee at the University of California, Irvine. To mimic the baseline conditions under which rats are evaluated following treatment with xenografted cell therapeutics, selected litters of RCS rats received daily dexamethasone injections (1.6 mg/kg i.p.) for a period of 2 weeks starting at the age of weaning (P21) and were also maintained on cyclosporine-A (Bedford Labs) administered in the drinking water (210 mg/L) from weaning age until the time of euthanasia. All procedures were carried out in accordance with the ARVO Statement for the Use of Animals in Ophthalmic and Vision Research.

Visual acuity

Visual acuity was estimated based on spatial frequency discrimination, tested at monthly intervals from P60-P180 using an Optomotry testing apparatus (Cerebral Mechanics). This device generates a virtual rotating cylinder consisting of a vertical sine wave grating presented in virtual 3-dimensional space on 4 computer monitors arranged in a square. Unrestrained rats were placed on a platform in the center of the square, where they tracked the grating with reflexive head movements. The spatial frequency of the grating was clamped at the viewing position by repeatedly recentering the ''cylinder'' on the head of the test subject. Acuity was quantified by increasing the spatial frequency of the grating using a psychophysics staircase progression until the optokinetic reflex was lost, thereby obtaining a maximum threshold. Due to the subjective nature of the assessment, all data were collected by a single researcher in an effort to eliminate potential bias.

Electroretinography recording

Retinal function was evaluated by full-field electroretinography (ERG) using a Ganzfeld stimulator at early (P43-46), mid (P59-61), and late (P90-93) time points. Additionally, selected animals were tested for an extended period up to age P180 in 1-month intervals. All animals were dark adapted overnight (>12 h) and prepared for testing under dim red light. Animals were anesthetized with a combination of Ketamine 70 mg/kg (Mylan Institutional Galway or equivalent) and Xylazine 3.5 mg/kg (Akorn or equivalent) delivered by a single intraperitoneal injection. Before the test, pharmacologic mydriasis was induced with 1 drop each topical Tropicamide 1% ophthalmic solution (Bausch & Lomb) and Phenylephrine 2.5% ophthalmic solution (Akorn). Animals were placed on a heated platform (37°C) to maintain a constant body temperature during measurement. ERGs were recorded from both eyes simultaneously using gold wire loops on each cornea as the active electrode with a drop of methylcellulose applied to the corneal surface for hydration during the testing procedure. Stainless steel needle electrodes (Rhythmlink) were placed subdermally at the base of the tail as ground and midline in the ventral aspect of the chin as the reference. Standard electroretinographic measurements were performed using the commercial Espion e3 recording unit coupled to the ColorDome Ganzfeld LED stimulator (Diagnosys LLC). The protocol included scotopic flash ERG at light intensities of 0.5 and 5 cds/m^2, photopic flash ERG at an intensity of 50 cds/m^2 after 10 min of light adaptation and 30 Hz photopic flicker at an intensity of 25 cds/m^2 (background of 30 cds/m^2). Oscillatory potentials were filtered using a bandpass filter set between 0.3 and 100 Hz.

Clinical examination

Immediately following ERG testing, with the pupil still dilated, tested eyes were inspected for media opacities using a portable slit lamp. Any eyes with substantial lesions of the cornea or lens were excluded from the study.

Retinal imaging (bright field & fluorescence angiography)

Color fundus images and fundus fluorescein angiography were obtained via a Micron III fundus imaging system (Phoenix Research Labs) with a rat objective. Before image acquisition, animals were pharmacologically dilated with topical mydriatics and anesthetized as described for ERG. Throughout the imaging procedure, methylcellulose was applied liberally to the cornea to maintain hydration and maximize optics. Following bright field image capture, a single fluorescein injection was delivered intraperitoneally

(0.1 mL of 10% AK Fluor/67 g BW) and fluorescent images were captured from the right eye for ~10 min post-injection using the same Micron III fundus imaging system. Fluorescent images were postprocessed to enhance brightness using Adobe Photoshop version CS6.

Histology

Animals were humanely euthanized by CO_2 asphyxiation. Globes were enucleated and postfixed in Davidson's solution for 48 h, then embedded in paraffin wax. For each eye, sagittal sections of 5 μm thickness were cut from lens to the optic nerve and routinely stained with hematoxylin and eosin (H&E). Selected slides from the peri-optic nerve area were imaged using a Nikon Eclipse Ti inverted research microscope (Melville) for morphological evaluation of retinal architecture and outer nuclear layer (ONL) thickness.

Statistical analysis

Statistical analyses were performed using JMP Genomics software version 5.1 for Windows. One-way analysis of variance (ANOVA) was performed to make the following comparisons between age-matched untreated and immunosuppressed RCS rats: body weights among same-sex rats, optokinetic threshold responses, and electroretinographic b-wave amplitudes. All variables were expressed as mean ± standard error of the mean. Differences were considered to be significant at $P < 0.05$.

Results

Functional comparison between immunosuppressed and untreated dystrophic RCS rats

To determine whether immunosuppressive treatment may have a preferential effect on functional measures of visual outcome, optomotor response (OR) thresholds and scotopic/photopic electroretinogram (ERG) responses were measured in untreated dystrophic RCS rats and dystrophic RCS rats under conditions of immunosuppression, with non-dystrophic Long Evans animals run as an age-matched comparison. Spatial frequency thresholds (mean ± standard error) for untreated dystrophic RCS rats at 60 days of age were 0.532 ± 0.006, significantly higher (ANOVA, $P < 0.0001$) than those measured in immunosuppressed RCS rats at 0.453 ± 0.008. At 90 days of age, OR responses were comparable between untreated RCS rats (0.281 ± 0.008)

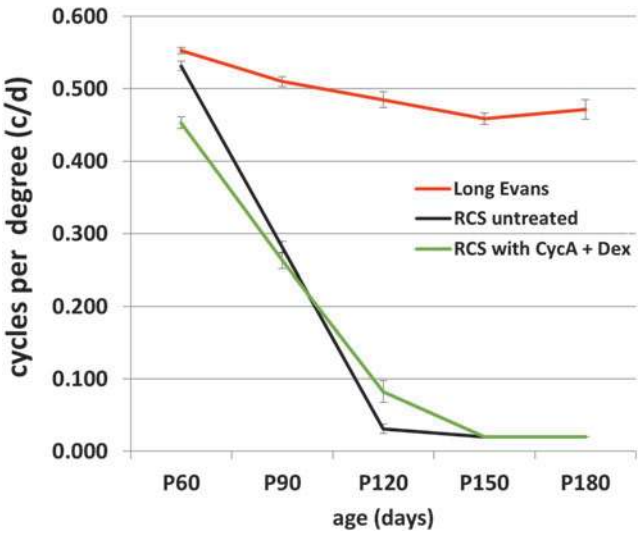

FIG. 1. OR thresholds in untreated dystrophic RCS rats (*black*), immunosuppressed dystrophic RCS rats (*green*), and untreated Long Evans rats (*red*). At 60 days of age, ORs in the group receiving systemic immunosuppression were significantly depressed versus untreated dystrophic and non-dystrophic controls. OR, optomotor response; RCS, Royal College of Surgeons.

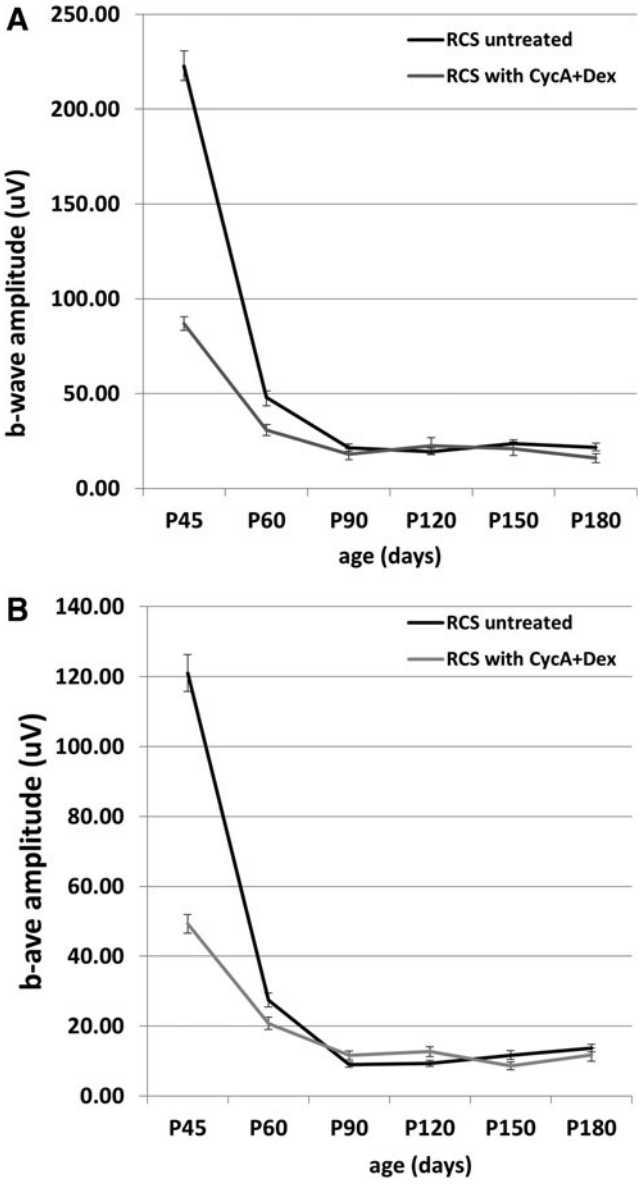

FIG. 2. ERG responses in untreated versus immunosuppressed dystrophic RCS rats. **(A)** Scotopic mixed rod-cone b-wave amplitudes were significantly depressed in immunosuppressed RCS rats (*blue*) at 45 and 60 days of age, versus untreated controls (*black*), but this disparity was no longer apparent at more advanced stages of retinal degeneration. **(B)** Photopic b-wave amplitudes were significantly depressed in immunosuppressed RCS rats at 45 and 60 days of age, versus untreated controls, but again this difference was not present at more advanced stages of retinal degeneration.

and immunosuppressed RCS rats (0.263 ± 0.011) (Fig. 1). Interestingly, at 120 days of age, immunosuppressed RCS rats exhibited significantly higher OR responses (ANOVA, $P < 0.0004$) compared with untreated dystrophic counterparts, whereas at all later time points evaluated, RCS animals in both groups fell below criterion threshold response levels.

Retinal function of animals at various stages of retinal degeneration was evaluated via recording of scotopic and photopic electroretinographic responses in immunosuppressed versus untreated dystrophic RCS rats (Fig. 2). Both a and b-waves were measured, with b-wave amplitude used as primary indicator of retinal function for the purposes of this study, as previously described in RCS rats.[13] Under scotopic conditions and with a flash intensity sufficient to elicit a mixed rod-cone response ($5\ \text{cds/m}^2$), b-wave amplitudes in immunosuppressed rats were significantly lower at P45 (ANOVA, $P < 0.0001$) and P60 (ANOVA, $P < 0.0015$) than those of untreated age-matched counterparts, but did not differ significantly once the disease had progressed to more advanced stages of retinal degeneration (Fig. 2A). The difference in b-wave amplitudes was not computed once responses fell below criterion threshold values defined as $<30\ \mu\text{V}$. Under photopic conditions, b-wave amplitudes of immunosuppressed RCS rats were again significantly lower at P45 (ANOVA, $P < 0.0001$) and P60 (ANOVA, $P < 0.0148$) than those of untreated counterparts, but did not differ significantly at subsequent time points (Fig. 2B).

As a measure of systemic health, body weights of male and female RCS rats receiving either no treatment or systemic immunosuppression were recorded on a gram scale at monthly intervals from 60 to 180 days of age (Fig. 3). Age-matched rats of the same sex were compared at each time point. Animals of both sexes receiving no immunosuppressive treatment had significantly higher body weights than their same-sex immunosuppressed counterparts at all time points for males (ANOVA, $P < 0.0001$) and up to P90 for females (ANOVA, $P < 0.001$), after which time their weights were comparable to untreated RCS rats.

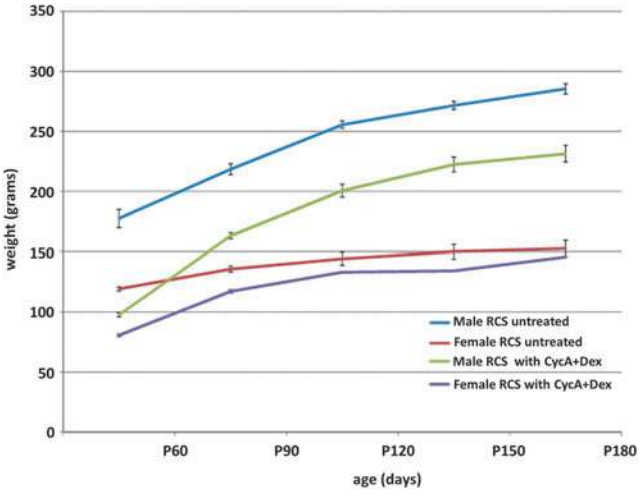

FIG. 3. Body weights of untreated male and female RCS rats compared over time with those of age-matched RCS rats undergoing systemic immunosuppression with cyclosporine A and dexamethasone. Untreated male (*blue*) and female (*red*) versus immunosuppressed male (*green*) and female (*purple*). Immunosuppression has a significant effect on weight for males, and females at earlier time points.

Histology and fundoscopic imaging: comparison of dystrophic RCS and non-dystrophic LE rats

Histological evaluation of untreated RCS rat retinas stained with H&E by light microscopy provided confirmation of dystrophic phenotype with progressive thinning of the ONL (Fig. 4). At postnatal age 21 days (P21), before the

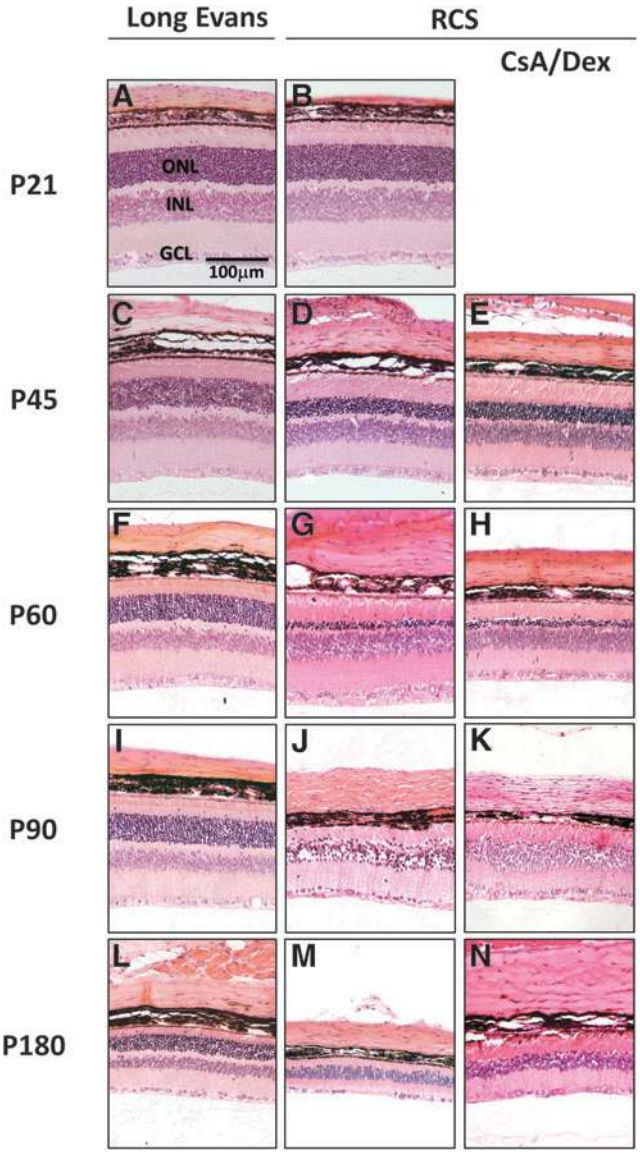

FIG. 4. Representative histological sections of dystrophic RCS rat retina over the course of retinal degeneration, including untreated **(B, D, G, J, M)**, immunosuppressed **(E, H, K, N)** and comparison with Long Evans rats **(A, C, F, I, L)**. The ONL of the RCS rat is $\sim$12 cell layers thick at 21 days of age **(B)**, when immunosuppression is initiated, but has degenerated to only 3 cell layers by 60 days of age **(G)**. A single broken layer is present at 90 days **(J)** with scattered to absent nuclei at time points examined thereafter **(M)**. There is no discernable difference in ONL thickness between untreated **(B, D, G, J, M)** and immunosuppressed **(E, H, K, N)** RCS groups at any age examined. In contrast, the ONL of the Long Evans strain remains thick out to P90 **(A, C, F, I)**, with moderate thinning to 8 cell layers at 180 days of age **(L)**. Scale bar applies to all images. GCL, ganglion cell layer; INL, inner nuclear layer; ONL, outer nuclear layer.

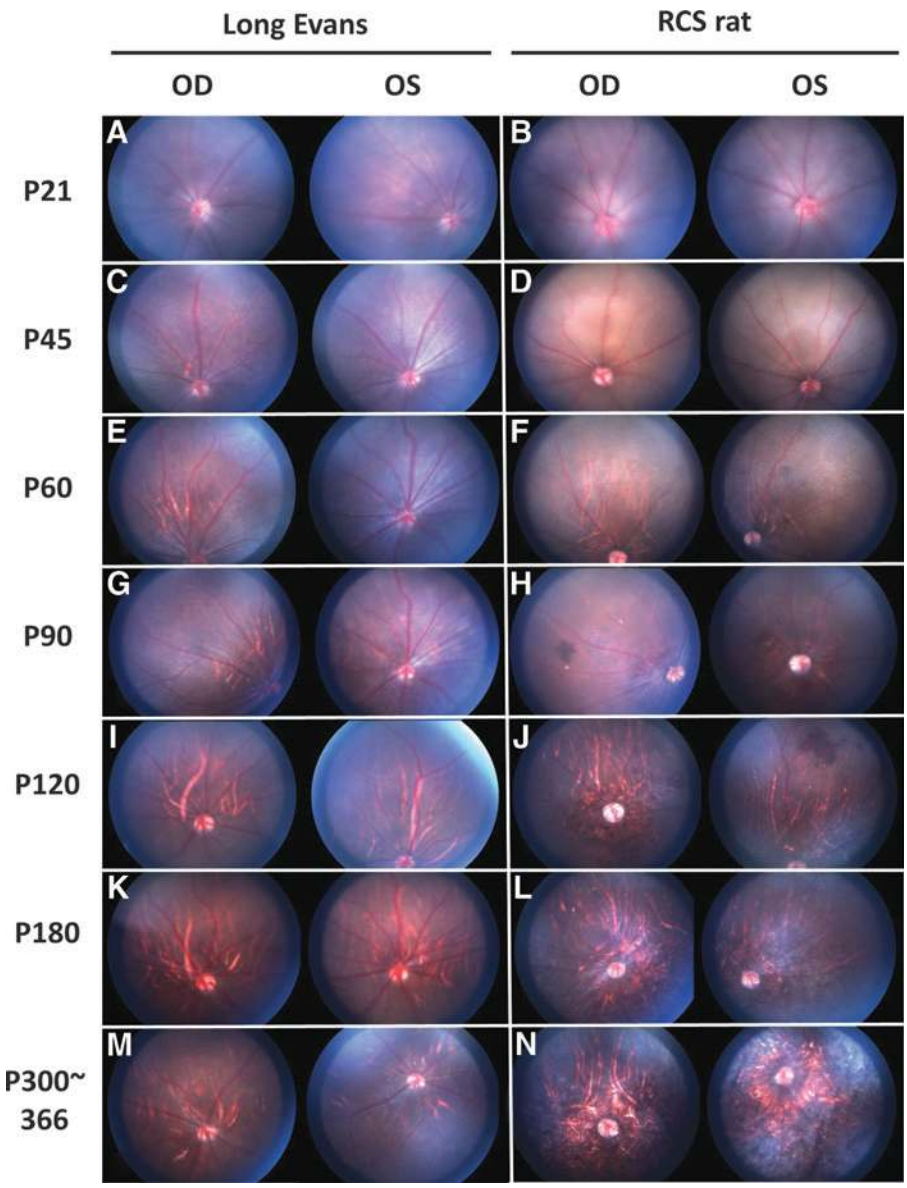

FIG. 5. Bright field fundus images of dystrophic RCS rats at various stages of retinal degeneration and comparison to Long Evans rats. The RCS fundus **(B, D, F, H, J, L, N)** shows evidence of progressive retinal degeneration characterized by attenuation of retinal vessels, migration of pigment into peripheral areas, and increased pallor of the optic disk. In contrast, in the Long Evans rat fundus **(A, C, E, G, I, K, M)**, underlying choroidal vessels become increasingly visible but no signs of retinal disease/degeneration are present even at advanced age.

onset of significant retinal changes, the ONL was ~12 rows of nuclei thick and normal retinal architecture was maintained. By 45 days of age (P45), ONL thickness had markedly decreased to 6–8 rows of nuclei. Pyknotic nuclei are present and the characteristic subretinal debris zone was evident between the ONL and the retinal pigment epithelial (RPE). At P60, further thinning of the ONL to ~3 rows was evident and there was notable effacement of the outer plexiform layer (OPL). By age P90, only a single broken layer of ONL remained. The OPL was nearly absent with the ONL and INL in close approximation. At more advanced stages of degeneration (P180) the ONL and OPL were absent. The INL had decreased in thickness and a degree of ganglion cell loss was also present. In comparison, retinal sections from an age-matched Long Evans rat retained ONL thickness out to P180 where there was some observed thinning down to 8 rows, but normal retinal architecture throughout.

In addition to histological processing, selected RCS rats were followed longitudinally to capture fundus changes associated with the disease pathology for comparison with the anatomical changes (Fig. 5). Age-matched Long Evans rats were also imaged to provide a nondegenerative comparison in a pigmented model, since nondystrophic RCS controls are, to our knowledge, no longer available. Fundus images of the dystrophic RCS rat retina at 21 days of age revealed healthy retinal vessels and optic nerve head against a dark background, comparable to the Long Evans rat fundus at the same age. By P90, the RCS rat exhibits marked attenuation of retinal arterioles and venules. Pigment clumping is seen in the peripheral retina, which is known to be associated with aberrant migration of RPE cells following loss of the ONL. Choroidal vessels are increasingly visible due to thinning and degeneration of overlying tissue, particularly the pigmented RPE layer. By P120, the pigment clumping associated with loss of the ONL extends into the ventral peripapillary region and the choroidal vasculature has become increasingly prominent, consistent with end-stage retinal degeneration.[14] In contrast, the mature Long Evans retina exhibits some visibility of underlying choroidal vessels, but without signs of retinal degeneration, even at an advanced age.

Fluorescein angiography was performed at various ages in RCS rats to document the progression of the vascular pathology associated with the retinal degeneration, in comparison to Long Evans controls (Fig. 6). At P90, and for all time points in Long Evans animals, fluorescein dye clearly defined the retinal vasculature, which appeared patent, of adequate caliber, and without evidence of leakage. Background fluorescence was uniform in appearance across the fundus, consistent with perfusion of the underlying choriocapillaris. By P120 and onward, the dystrophic RCS rats showed progressive loss of caliber in the retinal vessels and an increased tendency toward tortuosity. There was increasingly frequent evidence of microvascular pathology in the retinal circulation and the pattern of background fluorescence was markedly abnormal, consistent with changes deep to the retina, including patchy loss of the choriocapillaris and window defects in the RPE layer.

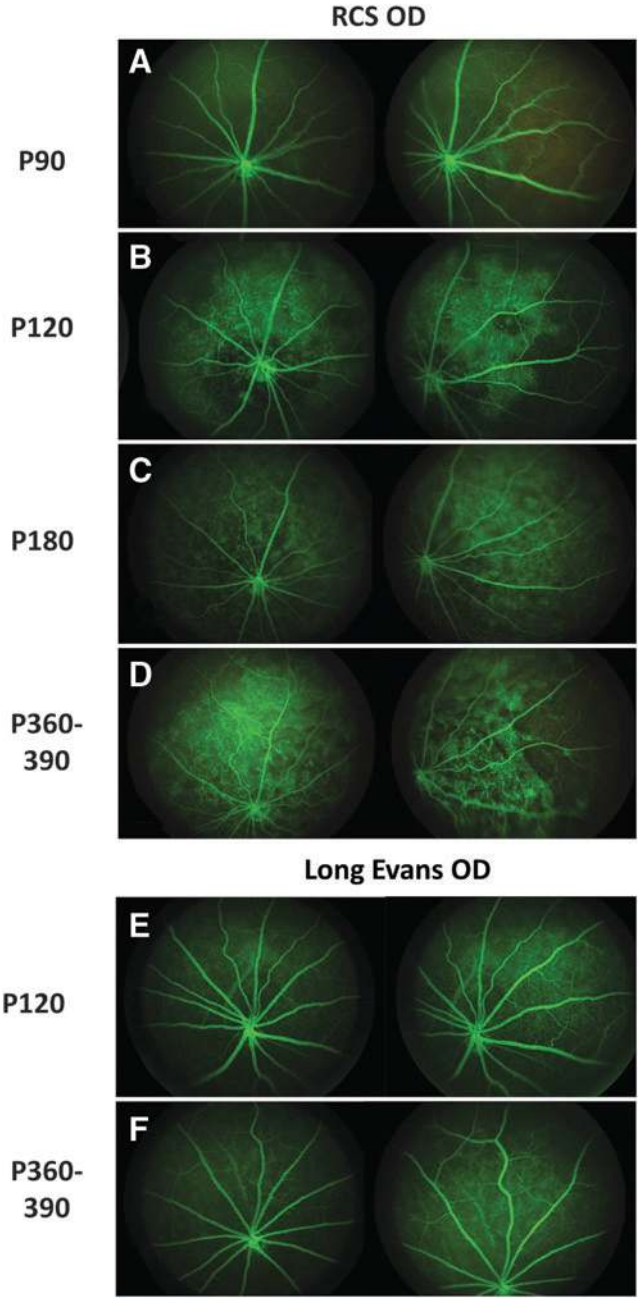

FIG. 6. Fluorescein angiography. Comparison of RCS rats **(A–D)** at various stages of retinal degeneration versus Long Evans rats **(E, F)**. In Long Evans animals, the dye remained confined to the intravascular compartment within the retina, with relatively uniform background fluorescence associated with the deeper choroidal circulation, at all time points examined **(E, F)**. The RCS animals showed similar findings at P90 **(A)**, while at later time points the retinal vessels showed evidence of attenuation and increased tortuosity, along with multiple local abnormalities **(B–D)**. In addition, there was a distinct non-uniformity in the pattern of background fluorescence from deeper structures.

Discussion

The RCS rat is a commonly employed rodent model of retinal degeneration, originally an attempt to understand RP[15] and more recently as a model for therapeutic intervention, including proof-of-concept studies for cell-based therapeutics. Enthusiasm for the RCS rat was lessened when it was determined that the causative defect was in the *MERTK* gene[16] and therefore differed from most cases of RP and, contrary to a direct role in rod photoreceptors, was related to ineffective phagocytosis at the level of the RPE. The model has enjoyed renewed popularity, however, as a well-characterized recipient for testing of a variety of cell-based interventions in the retina. Of note, *MERTK* is also expressed within the immune system, particularly by macrophages[17] but also reportedly by regulatory cells.[18] Successful testing of candidate human cell products in the RCS rat requires systemic immunosuppression of recipient animals, yet the effects of this treatment on visual function in this model had received little attention, despite the theoretical potential for interaction between the underlying defect and the immune system. Here, we provide evidence of altered visual function in RCS rats associated with immunosuppression, while expanding the range of baseline data available in this model.

The primary focus of this study was establishing baseline data during development of a proof-of-concept model for testing a human retinal progenitor cell product as potential therapy for the orphan blinding disease RP. The OR values obtained for untreated dystrophic RCS rats fell between those published in previous reports.[19,20] In 1 report, RCS rats treated with cyclosporine A only (same dose and method of administration as current study) were reported to achieve OR values of 0.3 cycle/degree (c/d) at P90, comparable to those reported here for both untreated and immunosuppressed rats.[21] The lack of disparity between untreated and immunosuppressed groups at P90 may reflect the advanced stage of degeneration and the relatively low number of photoreceptors available to generate a tracking response. Consistent with this concept, untreated RCS rats demonstrated significantly higher spatial frequency thresholds than their immunosuppressed counterparts at the earliest time point evaluated (P60), and this effect became less apparent as the disease progressed to more advanced stages of degeneration (P90). Also, consistent with this were the results of ERG testing.

Substantial work has been done by others to characterize the electroretinogram (ERG) responses of RCS rats[22] and utilize this test in translational studies to evaluate the efficacy of xenografted cell-based therapeutics with respect to

improvements in functional outcomes and to characterize the nature of the rescue achieved.[20,23] Studies published to date, however, have not considered the impact of immunosuppressive therapy on retinal function in this model. Consistent with the trends seen from the OR testing described above, we found an immunosuppression-associated reduction in b-wave amplitudes at P45 and P60 time points, under scotopic conditions using a flash intensity sufficient to elicit a mixed rod-cone response (5 cds/m^2). Again, the magnitude of the difference versus controls diminished with time and was no longer significant once the disease had progressed to more advanced stages of retinal degeneration (P90). Measurement of the photopic b-wave yielded the same result.

The disparity in body weights associated with dexamethasone and cyclosporine A administration observed here was not unexpected. Cyclosporine A was shown to decrease body weights when administered to rats via induction of both hypophagia and protein catabolism.[24,25] Dexamethasone at high doses has been shown to cause hypophagia and weight loss in rats.[26] With respect to sex differences, anatomical studies have demonstrated that female rats have larger adrenal and anterior pituitary glands than males of the same strain[27] and higher corticosterone levels under both stressed and nonstressed conditions.[28,29] As a result of these anatomical and physiological differences, it is possible that females may produce higher levels of ACTH, which are suppressed to a lesser degree by administration of equivalent doses of dexamethasone compared with male littermates, thereby mitigating the effects of hypophagia in the mature rat.

Previous work by LaVail and Battelle[30] described the progression of retinal degeneration in the RCS rat, although the details of the timing differ substantially between the pink-eyed and brown-eyed strains. The use of P21 for initiating administration of therapeutic agents corresponds to weaning and precedes the onset of substantial changes. Our findings of a 3-layer ONL at 60 days of age, which progresses to a single broken layer of nuclei by 90 days of age, is expected and comparable to previous reports in the brown-eyed strain.[20] Analysis of H&E-stained sections in this study did not reveal any anatomical differences between immunosuppressed and untreated dystrophic RCS groups.

The fundoscopic changes observed tended to mimic the classic signs of RP in humans, including intraretinal ''bone spicule'' pigmentation, retinal arteriolar attenuation, and waxy pallor of the optic disk,[31] despite the difference in underlying etiology. To the authors' knowledge, there are no other reports detailing the fundoscopic appearance of the pigmented dystrophic RCS rat retina over the time course of retinal degeneration. Previous studies focused on the more rapidly degenerating pink-eyed strain[32] or have used imaging modalities that precluded a detailed demonstration of the degenerative changes.[14] The comprehensive time course of fundoscopic changes documented here may provide a helpful reference for other workers in the field. Fluorescein angiography on patients with RP is known to show vascular attenuation secondary to the degenerative process[33] and, at later stages of disease, migration of RPE cells into the retina is associated with formation of abnormal retinal vascular complexes. Similar processes appear to be taking place in the RCS retina and the angiographic data presented here are consistent with that interpretation.

In summary, the data presented here indicate that the possibility of visual changes relating to immunosuppressive treatment deserves consideration when working in the RCS model. This extends to both experimental design and interpretation of the resulting data. In general, the changes observed were most evident at earlier time points, corresponding to the most active phases of photoreceptor loss. The frequently used P90 time point, at which time the ONL is largely gone, no longer exhibited significant differences between treatment groups, perhaps due to the advanced stage of the degenerative process. This study did not identify the source of the visual deficit and the underlying retinal anatomy was similar between immunosuppressed and untreated dystrophic RCS groups. The absence of media opacities on clinical examination argues against something as simple as steroid-induced cataract. Because of the association with both ERG amplitude and the active phase of photoreceptor cell loss, but not ONL thickness, it is tempting to invoke the possibility of immune-related impairment of subcellular processes such as debris removal and perhaps synaptic remodeling, although this is entirely speculative. Future work will be needed to provide more detail on the effect itself and to elucidate responsible mechanisms, including the relative contribution of cyclosporine and steroid components. In the meantime, those using the RCS model for functional readouts on xenografts should be aware of the possibility that the resulting data may in some cases underrepresent the optimal therapeutic potential of their product.

Acknowledgments

The authors would like to thank Tim Hou for technical assistance with ERG, Jennifer Eschebal-Chen for technical assistance with optomotor testing and histology, and Aaron Tagger for article review. These studies were supported by a grant from CIRM (Award No. DR2A-05739).

Author Disclosure Statement

Henry Klassen and Jing Yang have an equity interest in jCyte, a company that may potentially benefit from the research results, and also serve on the company's Board. The terms of this arrangement have been reviewed and approved by the University of California, Irvine in accordance with its conflict of interest policies.

References

1. Buchholz, D.E., Pennington, B.O., Croze, R.H., et al. Rapid and efficient directed differentiation of human pluripotent stem cells into retinal pigmented epithelium. *Stem Cells Transl. Med.* 2:384–393, 2013.
2. Reardon, S., and Cyranoski, D. Japan stem-cell trial stirs envy: researchers elsewhere can't wait to test iPS cells in humans. *Nat. News.* 513:287–288, 2014.
3. Klassen, H. Stem cells in clinical trials for treatment of retinal degeneration. *Expert Opin. Biol. Ther.* 16:7–14, 2015.
4. Lund, R.D., Wang, S., Klimanskaya, I., et al. Human embryonic stem cell-derived cells rescue visual function in dystrophic RCS rats. *Cloning Stem Cells.* 8:189–199, 2006.
5. Schwartz, S.D., Hubschman, J.P., Heilwell, G., et al. Embryonic stem cell trials for macular degeneration: a preliminary report. *Lancet.* 379:713–720, 2012.

6. Schwartz, S.D., Regillo, C.D., Lam, B.L., et al. Human embryonic stem cell-derived retinal pigment epithelium in patients with age-related macular degeneration and Stargardt's macular dystrophy: follow-up of two open-label phase 1/2 studies. *Lancet.* 385:509–516, 2015.
7. DiLoreto, Jr., D., del Cerro, C., and del Cerro, M. Cyclosporine treatment promotes survival of human fetal neural retina transplanted to the sub retinal space of the light-damaged Fischer 344 rat. *Exp. Neurol.* 140:37–42, 1996.
8. Sakaguchi, D.S., Van Hoffelen, S.J., and Theusch, E. Transplantation of neural progenitor cells into the developing retina of the Brazilian opossum: an in vivo system for studying stem/progenitor cell plasticity. *Dev. Neurosci*. 26: 336–345, 2004.
9. Warfvinge, K., Kiilgaard, J.F., Lavik, E.B., et al. Retinal progenitor cell xenografts to the pig retina: morphologic integration and cytochemical differentiation. *Arch. Ophthalmol*. 123:1385–1393, 2005.
10. Warfvinge, K., Kiilgaard, J.F., and Klassen, H. Retinal progenitor cell xenografts to the pig retina: immunological reactions. *Cell Transplant.* 15:603–612, 2006.
11. Coffey, P.J., Girman, S., and Wang, S.M. Long-term preservation of cortically dependent visual function in RCS rats by transplantation. *Nat. Neurosci*. 5:53–56, 2002.
12. Charreau, B., Coupel, S., Goret, F., Pourcel, C., and Soulillou, J.P. Association of glucocorticoids and cyclosporine A or rapamycin prevents E-selectin and IL-8 expression during LPS- and TNFα-mediated endothelial cell activation. *Transplantation.* 69:945–953, 2000.
13. Sauvé, Y., Lu, B., and Lund, R.D. The relationship between full field electroretinogram and perimetry-like visual thresholds in RCS rats during photoreceptor degeneration and rescue by cell transplants. *Vis. Res.* 44:9–18, 2004.
14. Herron, W.L., Riegel, B.W., Brennan, E., and Rubin, M.L. Retinal dystrophy in the pigmented rat. *Invest. Ophthalmol.* 13:87–94, 1974.
15. Bok, D., and Hall, M.O. The etiology of retinal dystrophy in RCS rats. *Invest. Ophthalmol. Vis. Sci*. 8:649–650, 1969.
16. D'Cruz, P.M., Yasumura, D., Weir, J., et al. Mutation of the receptor tyrosine kinase gene Mertk in the retinal dystrophic RCS rat. *Hum. Mol. Genet.* 9:645–651, 2000.
17. Ling, L., and Kung, H.J. Mitogenic signals and transforming potential of Nyk, a newly identified neural cell adhesion molecule-related receptor tyrosine kinase. *Mol. Cell. Biol*. 15:6582–6592, 1995.
18. Bernsmeier, C., Pop, O.T., Singanayagam, A., et al. Patients with acute-on-chronic liver failure have increased numbers of regulatory immune cells expressing the receptor tyrosine kinase MERTK. *Gastroenterology*. 148: 603–615.e14, 2015.
19. McGill, T.J., Lund, R.D., Douglas, R.M., et al. Preservation of vision following cell-based therapies in a model of retinal degenerative disease. *Vis. Res*. 44:2559–2566, 2004.
20. Wang, S., Lu, B., Girman, S., et al. Morphological and functional rescue in RCS rats after RPE cell line transplantation at a later stage of degeneration. *Invest. Ophthalmol. Vis. Sci*. 49:416–421, 2008.
21. Wang, S., Lu, B., Girman, S., et al. Non-invasive stem cell therapy in a rat model for retinal degeneration and vascular pathology. *PLoS One.* 5:e9200, 2010.
22. Pinilla, I., Lund, R.D., and Sauve, Y. Contribution of rod and cone pathways to the dark-adapted electroretinogram (ERG) b-wave following retinal degeneration in RCS rats. *Vis. Res.* 44:2467–2474, 2004.
23. Smith, A.J., Schlichtenbrede, F.C., Tschernutter, M., et al. AAV-mediated gene transfer slows photoreceptor loss in the RCS rat model of retinitis pigmentosa. *Mol. Ther.* 8: 188–195, 2003.
24. Farthing, J.G., and Clark, M.L. Nature of the toxicity of cyclosporine in the rat. *Biochem. Pharmacol.* 30:3311–3316, 1981.
25. Jaramillo-Juárez, F., Rodríguez-Vázquez, M.L., Namorado, M.C., Martín, D., and Reyes, J.L. Acidosis and weight loss are induced by cyclosporin A in uninephrectomized rats. *Pediatr. Nephrol*. 14:122–127, 2000.
26. Beatty, P.A., Beatty, W.W., Bowman, R.E., and Gilchrist, J.C. The effects of ACTH, adrenalectomy and dexamethasone on the acquisition of an avoidance response in rats. *Physiol. Behav*. 5:939–944, 1970.
27. Swanson, H.E., and van der Werff-ten Bosch, J.J. Sex differences in growth of rats, and their modification by a single injection of testosterone propionate shortly after birth. *J. Endocrinol*. 26:197–207, 1963.
28. Ader, R. Effects of early experiences on emotional and physiological reactivity in the rat. *J. Comp. Physiol. Psychol.* 66:264–268, 1968.
29. Kitay, J.I. Sex differences in adrenal cortical secretion in the rat. *Endocrinology.* 68:818–824, 1961.
30. LaVail, M.M., and Battelle, B.A. Influence of eye pigmentation and light deprivation on inherited retinal dystrophy in the rat. *Exp. Eye Res.* 21:167–192, 1975.
31. Kanski, J. Fundus dystrophies. In: Kanski, J., Sehmi, K., Bolton, A., eds. *Clinical Ophthalmology: A Systemic Approach, 6th ed.* Philadelphia: Elsevier; 2008; pp. 663–694.
32. Satoh, T., and Yamaguchi, K. Ocular fundus abnormalities detected by fluorescein and indocyanine green angiography in the Royal College of Surgeons dystrophic rat. *Exp. Anim.* 49:275–280, 2000.
33. Milam, A.H., Li, Z.Y., and Fariss, R.N. Histopathology of the human retina in retinitis pigmentosa. *Prog. Retin Eye Res*. 17:175–205, 1998.

Received: November 2, 2015
Accepted: January 21, 2016

Address correspondence to:
Jing Yang
Assistant Professor
Gavin Herbert Eye Institute
Stem Cell Research Center
University of California, Irvine
Sue & Bill Gross Hall
Room 2006, 845 Health Sciences Road
Irvine, CA 92697 1705

E-mail: yjbell@gmail.com

Henry Klassen
Associate Professor
Gavin Herbert Eye Institute
Stem Cell Research Center
University of California, Irvine
Sue & Bill Gross Hall
Room 2006, 845 Health Sciences Road
Irvine, CA 92697 1705

E-mail: hklassen@uci.edu